

SOUTH POLAR LAYERED DEPOSITS NEAR-SURFACE PROPERTIES INFERRED FROM A DATED IMPACT CRATER. M.E. Landis¹, A.S. McEwen², I.J. Daubar³, P.O. Hayne¹, S. Byrne², C.M. Dundas⁴, S.S. Sutton², A. Britton⁵, K.E. Herkenhoff⁴. ¹Laboratory for Atmospheric and Space Physics, University of Colorado, Boulder, CO (margaret.landis@lasp.colorado.edu), ²Lunar and Planetary Laboratory, University of Arizona, Tucson, AZ, ³Jet Propulsion Laboratory, California Institute of Technology, Pasadena, CA, ⁴Astrogeology Science Center, USGS, Flagstaff, AZ, ⁵Johnson Space Center, Houston, TX.

Introduction: Mars' Polar Layered Deposits (PLDs) contain tantalizing clues to deciphering Mars' climate history. Previous studies have detected recurring patterns in the alternating layers of ice and dust [e.g., 1, 2] and made estimates of the accumulation rates required to replicate them [e.g., 3, 4]. Orbital data from several Mars years have made significant progress in constraining the inter-annual variations in the seasonal CO₂ ice and other key controls on the mass balance of the PLDs [e.g., 5]. From thermal modeling and martian obliquity models, it appears unlikely that the current North PLD (NPLD) could have survived beyond 5 Myr before the present [6-8], though crater age estimates for the South PLD (SPLD) surface are $\gg 5$ Myr [9-11].

Multiple lines of evidence indicate the SPLD formed in large depositional events with long erosional hiatuses. These include stratigraphic relationships from geologic mapping [12] and scarp protrusion analysis [13], and the higher bulk dust content than the NPLD, as inferred from gravity [14]. Characterizing the upper meters of the SPLD will help determine the depth and composition of the SPLD sublimation lag, and therefore the length of the SPLD's current accumulation hiatus (and support the orders of magnitude older surface age than the NPLD).

We report inferred SPLD surface properties from an observed new impact crater, ~18 m in diameter, detected between Context Camera (CTX) observations acquired in July and September 2018 at ~81.5° S, 41° E. We infer a minimum ~3 m deep buried sublimation lag deposit at this location.

SPLD impact crater features: While the detection of dated (e.g., a before and after impact image, usually from CTX, constraining the formation time) impact events has been common in the dusty regions of Mars [15, 16], this is the first documented detection of a new, dated impact on the SPLD. This ~18 m impact was imaged by HiRISE in October 2018 (Figure 1) after detection by CTX in September.

The first HiRISE observation of the crater occurred while CO₂ frost was still present (Figure 1, left panel). Lighter patches can be seen adjacent to dark ejecta which could be caused by ejecta material scouring the surface. Overall, the crater ejecta resembles that of impacts into ice-free targets in the equatorial regions of Mars [16-18].

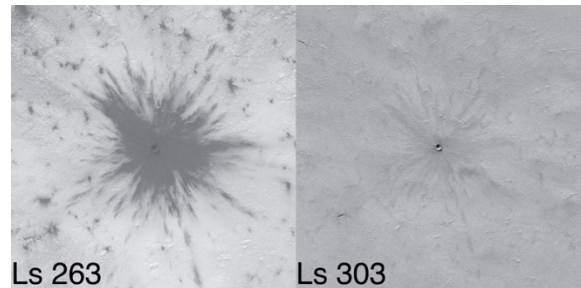


Figure 1. The ~18m diameter new impact crater in two HiRISE images (ESP_057152_0985 & ESP_057970_0985), one with (left) and without (right) seasonal frost coverage.

The PLDs are ice-rich, and at a temperature where the effective yield strength may cause systematically larger diameter craters compared to impacts into only lithic material [e.g., 19]. The ~18 m diameter of this crater is within range of the diameters of ice-exposing mid-latitude craters (~2-24 m individual craters) [17] and new, dated craters (~2-34 m) [18]. While there is only one current example, the dated SPLD impact diameter is not significantly larger than others into lithic targets and does yet indicate that the SPLD target strength varies dramatically from the mid-latitudes regions of Mars.

The elevation profiles from a HiRISE digital terrain model (DTM) (Figure 2) show that this crater has a simple bowl-shape, and lacks topographic features suggestive of an effective strength difference in the upper few meters of the surface [e.g., 20]. The crater has a depth-to-diameter ratio (d/D) of ~0.15-0.18. The mean d/D of dated impacts (all primary craters or primary crater clusters) into lithic targets is ~0.23, with a large range [18]. Daubar et al. [18] calculated the maximum d/D ratio for a parabolic crater with walls at a dynamic angle of repose of ~35° would be ~0.175. The new SPLD impact d/D ratio and interior morphology are consistent with a primary impact crater into single effective strength target.

Persistent dark ejecta and implications for grain size: Even after the surrounding terrain had defrosted (Figure 1), the inner, continuous ejecta of this crater remained dark compared to the defrosted SPLD surface. This could be caused by a grain size difference between the ejecta blanket and the surrounding terrain. While other factors like surface

roughness or compaction could contribute to this, here we primarily explore grain size as a cause.

In order to estimate the grain size difference between ejecta and surroundings, we first calculated an average I/F value from the HiRISE images in representative sections of the dark ejecta and surrounding, unaffected SPLD surface (Figure 3). To interpret these I/F results in terms of grain size, we used a radiative transfer model from [21], optical constants for Mars dust from [22] and Mie scattering theory. We assume the particle size-distribution follows a modified gamma distribution [23]. The model I/F vs. mode radius is plotted in Figure 3. In order to replicate the differences in measured I/F, the ejecta would have to contain slightly larger dust particles than the surrounding defrosted SPLD surface. This suggests that larger-grained dust was preferentially preserved, possibly as smaller particles were removed by winds.

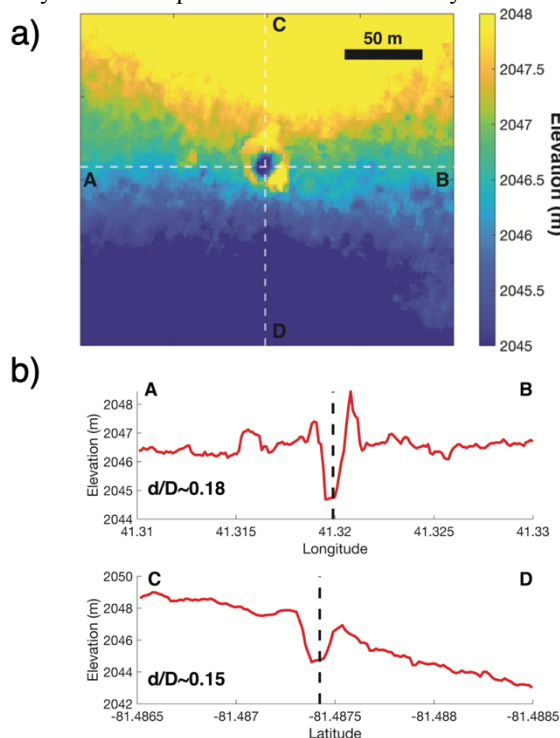


Figure 2. a) The HiRISE DTM (north is up) and b) depth profiles showing the calculated depth/diameter ratio for the new, dated SPLD impact.

Could there have been water ice in the ejecta blanket?: We know that the bulk PLD are rich in water ice, the ice stability models indicates it should be present at shallow depths near the poles [e.g., 24]. Though early summer color images show a small, bluer area, this crater does not have a bright ejecta blanket like those at mid-latitudes [17]. We estimated the water sublimation rate to determine if a water ice ejecta layer could have sublimated between crater

formation and imaging by CTX (max. ~2 months) and HiRISE (max. ~3 months). During this time, CO₂ frost was present and likely fixed the surface temperature at ~150 K. A maximum of ~50-80 μm m⁻² of water ice could have sublimated before the crater was imaged by CTX and HiRISE. Therefore, sublimation would have only effectively removed little water ice from the ejecta.

We will refine these estimates using Mars Climate Sounder (MCS) data and estimate the resulting ice/regolith mixing ratio for the upper few meters of the SPLD. Regardless of uncertainties in this sublimation, however, this crater exposed far less water ice than those at the mid-latitudes [17].

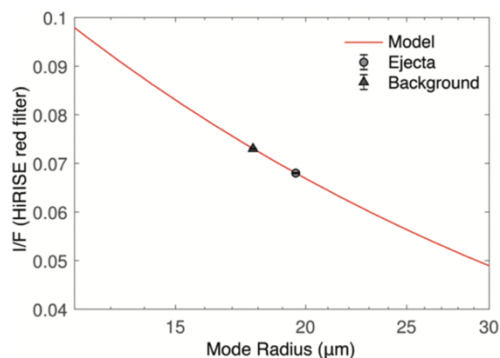


Figure 3. I/F calculated in the HiRISE red filter wavelength range for different particle sizes. Statistical uncertainties in the I/F measurement are small compared to uncertainties in the model, and are smaller than the symbols plotted above.

Acknowledgements: The authors wish to thank the Mars Reconnaissance Orbiter project and HiRISE team, including the HiTS/CIPPs on cycle during imaging, the HiRISE DTM lab, and Daniel Robinson.

References: [1] Milkovich, S.M., et al. *JGR*, 2005. **110**(E1). [2] Becerra, P., et al., *JGR:Planets*, 2016. **121**(8) [3] Fishbaugh, K.E. and C.S. Hvidberg, *JGR*, 2006. **111**(E6). [4] Hvidberg, C.S., et al., *Icarus*, 2012. **221**(1) [5] Piqueux, S., et al., *Icarus*, 2015. **251** [6] Jakosky, B.M., et al., *JGR: Planets*, 1995. **100**(E1). [7] Laskar, J., et al., *Nature*, 2002. **419**. [8] Levrard, B., et al., *JGR:Planets* 2007. **112**(E6). [9] Koutnik, M., et al, *JGR: Planets*, 2002. **107**(E11) [10] Herkenhoff, K. and J.J. Plaut, *Icarus*, 2000. **144**(2) [11] Landis, M.E., et al., *Amazonian Climate Workshop*. LPI Contributions, 2019. **2089**. [12] Kolb, E.J. and K.L. Tanaka, *Mars*, 2006. [13] Becerra, P., et al., *GRL*, 2019. **46**(13): p. 7268-7277. [14] Zuber, M.T., et al., *Science*, 2007. **317**(5845) [15] Malin, M.C., et al., *Science*, 2006. **314**(5805). [16] Daubar, I.J., et al., *Icarus*, 2013. **225**(1) [17] Dundas, C.M., et al., *JGR:Planets*, 2014. **119**(1) [18] Daubar, I.J., et al., *JGR:Planets*, 2014. **119**(12) [19] Landis, M.E., et al., *GRL*, 2016. **43**(7). [20] Quaide, W.L. and V.R. Oberbeck, *JGR*, 1968. **73**(16). [21] Wiscombe, W.J. and S.G. Warren, *J. of Atm. Sci.*, 1980. **37**(12). [22] Wolff, M.J. and R.T. Clancy, *JGR:Planets*, 2003. **108**(E9). [23] Hayne, P.O., et al., *JGR:Planets*, 2012. **117**(E8). [24] Mellon, M.T., et al., *Icarus*, 2004. **169**(2): p. 324-340